© JUL 2026 | IRE Journals | Volume 10 Issue 1 | ISSN: 2456-8880
DOI: https://doi.org/10.64388/IREV10I1-1719856

Dynamic Behavior of Euler Bernoulli beam of Arbitrary Number of Variable Elastic K-Stiffness under a Partially Distributed Moving Load

IBIKUNLE ALBERT IDOWU[1], RAFIU BOLAJI ADEGBOLA[2], JOSHUA OLUWAGBENGA AJILORE[3], CHRISTIANA ILUNO[4], MATTHEW IWADA EKUM[5]

[1,3,4,5]Department of Mathematical Sciences, College of Basic Sciences, Lagos State University of Science and Technology, Ikorodu. Lagos, Nigeria

[2]Department of Mathematics, Lagos State University, Ojo, Nigeria

Abstract-* Modern transport systems have undergone significant advancements, necessitating improved structural models for analyzing the dynamic response of beams under moving loads. This study investigated the response of an Euler-Bernoulli beam with variable elastic K-stiffness subjected to a partially distributed moving mass. The beam is simply supported, and the moving mass travels at a constant velocity. A mathematical model is developed, incorporating the effects of stiffness variation, inertia, and load distribution. The governing equation is solved using an analytical-numerical approach with Maple. Results indicate that the effect of a moving mass is more significant than that of a moving force, influencing beam deflections based on stiffness variations. These findings provide insights into optimizing beam designs for transport and structural applications.

Keywords: Beam Deflection; Elastic K-Stiffness; Mass Variation; Moving Load; Structural Vibration

I. INTRODUCTION

The dynamic behavior of beams under moving loads has long been a critical area of research in structural mechanics, particularly for applications where structures must endure time-varying forces [1]. The Euler-Bernoulli beam theory, one of the most fundamental models in this field, assumes that beams bend under applied loads while neglecting shear deformations and the rotational inertia of beam elements. Though the Euler-Bernoulli model is effective for many practical problems, it becomes significantly more complex when considering beams with varying elastic properties and the effect of moving loads. This complexity is further magnified when the beam is subjected to a partially distributed moving load, a scenario that commonly occurs in real-world applications, such as railways, bridges, and transportation infrastructure [2-4].

The study of Euler-Bernoulli beams with variable elastic properties, particularly those with K-stiffness that varies along the beam's length, plays a crucial role in modern engineering [5]. These beams are essential in representing structures made from materials whose stiffness is not constant but changes due to factors such as material heterogeneity or environmental conditions. K-stiffness, in such cases, is often modeled as a function of spatial coordinates along the beam's length, offering a more precise representation of real-world scenarios [6]. This approach allows for better understanding and prediction of the behavior of structures subjected to dynamic loads and varying material properties [7].

When a moving load is applied to a beam, the dynamic behavior becomes significantly more complicated. The load does not remain fixed at a single point but instead moves along the length of the beam, continuously altering the forces and deformations the beam experiences [8]. The nature of the load itself is another important factor; a moving load is often partially distributed along the length of the beam, rather than being a point load. This partially distributed load can vary in magnitude, intensity, and distribution along the beam, making the analysis more challenging. The combination of these variables, variable stiffness and a partially distributed moving load introduces intricate dynamics that are critical for understanding the behavior of structures under real-world conditions [9].

Many studies [4,8,10-16] have been conducted to investigate the dynamic behavior of beams under moving loads. Early works focused on the analysis of beams with constant stiffness under point loads, which could be modeled using classical beam theory. However, as engineering challenges evolved, there was an increasing need to account for variable material properties and complex loading scenarios. Researchers [8,17-21] have developed various mathematical and computational models to capture the dynamic responses of beams with spatially varying stiffness. These models involve partial differential equations that describe the beam's deflection, velocity, and acceleration as a function of both time and spatial position.

The effects of a moving load on a beam's dynamic response can be particularly severe. In certain cases, resonance phenomena can occur when the frequency of the moving load matches the natural frequency of the beam. This can lead to large deflections and potential structural failure. This phenomenon is well-documented in the literature, and much research has been dedicated to understanding the conditions under which resonance can occur and how it can be mitigated. In beams with variable stiffness, the resonant frequencies themselves change along the beam's length, adding further complexity to the analysis [22-23].

For beams with variable stiffness, it is essential to model the stiffness variation accurately. The stiffness function, often denoted as K(x), where x represents the position along the beam, can take various forms [24-26]. In many cases, the variation is linear, exponential, or polynomial, depending on the physical properties of the material and the geometry of the beam. The inclusion of variable stiffness introduces a non-uniformity in the distribution of the beam's flexural rigidity, which affects both the natural frequencies and the mode shapes of the beam. This is a critical consideration in the design of structures like bridges, where the stiffness of materials can vary due to aging, wear, or environmental conditions [27-29].

Additionally, the nature of the load itself plays a significant role in the beam's response. A moving load is typically characterized by both its magnitude and its position along the beam, as well as its velocity [30-31]. The velocity of the load introduces time-dependent effects, which must be carefully considered in the analysis. In many cases, the moving load may be partially distributed along the beam, further complicating the problem. Such loads can be modeled as a function of position along the beam and time, where the load distribution changes dynamically as the load moves [32].

The interactions between the variable stiffness of the beam and the moving load have been explored in numerous studies [33-43]. Numerical methods, such as finite element analysis (FEA), have become increasingly popular for simulating the dynamic behavior of such systems. These methods allow for the incorporation of complex boundary conditions, variable material properties, and time-varying loads, providing more accurate and detailed results than traditional analytical methods. In finite element modeling, the beam is discretized into small elements, and the governing equations are solved for each element, taking into account the varying stiffness and the moving load [44].

In addition to numerical methods, experimental approaches have also been used to validate the theoretical models. Laboratory tests on beam specimens with variable stiffness and moving loads provide valuable data that can be compared to the predictions made by numerical models. These tests help to refine the models and improve their accuracy, especially when dealing with real-world materials and loading conditions. Experimental results can also reveal unexpected behaviors, such as non-linearities or unexpected resonance effects, that may not be captured in theoretical models [45-46].

The study of partially distributed moving loads on beams has applications in many fields [47-51]. In civil engineering, bridges and overpasses must be designed to withstand the dynamic effects of moving vehicles, which exert varying loads on the structure as they pass. Similarly, railway tracks must be designed to handle the effects of trains passing over them, which can result in significant dynamic forces. In these cases, the load is often partially distributed along the length of the beam, and the stiffness of the beam may vary due to factors such as wear, aging, or different materials used in different sections of the structure [52].

The analysis of such systems is crucial for ensuring the safety and longevity of infrastructure. Understanding the dynamic behavior of beams under moving loads, engineers can better predict the performance of structures under real-world conditions and design them to withstand these forces. Furthermore, by considering the effects of variable stiffness and partially distributed moving loads, engineers can develop more efficient designs that minimize material usage and reduce costs without sacrificing safety or performance [53-54].

The dynamic behavior of Euler-Bernoulli beams with arbitrary numbers of variable elastic K-stiffness under partially distributed moving loads is a complex and highly relevant area of research. The combination of variable stiffness, moving loads, and time-varying effects introduces significant challenges in both the theoretical analysis and numerical simulation of these systems. As such, ongoing research in this field is essential for advancing our understanding of beam dynamics and improving the design of structures subjected to dynamic loading conditions. Future work will continue to refine mathematical models, improve numerical methods, and validate these models through experimental testing, ensuring that engineers can design safer, more efficient structures capable of withstanding the challenges of modern infrastructure [55-56].

The need to study the behavior of structures under moving loads with variable velocity has become increasingly important. Real-world applications such as acceleration and braking of automobiles on roadways and bridges, aircraft takeoff and landing on runways, and braking and acceleration forces in railway bridge calculations highlight the necessity of understanding these dynamic effects. Addressing these challenges will contribute to the development of more accurate predictive models and improved structural designs, ensuring the safety and efficiency of transportation and infrastructure systems. The study would be beneficial to civil engineers, construction professionals, transportation agencies, researchers in structural dynamics, manufacturers of damping devices, and environmental engineers. They can apply the findings to improve infrastructure design, enhance the resilience of beams under dynamic loads, and develop more effective damping systems for safer, durable structures.

II. MATERIALS & METHODS

2.1 The Old Model of Oni and Awodola [57]

Consider a long slender beam as shown in figure 1 subjected to transverse vibration. The free body diagram of an element of the beam is shown in figure 2, where, $M(x,t)$ is the bending moment, is the $V(x,t)$ shear force, and $f(x,t)$ is the external force per unit length of the beam. Since the inertia force acting on the element of the beam is $\rho A dx \frac{\partial^2 w(x,t)}{\partial t^2}$

Balancing the force in z direction gives:

$$-(V+dV)+f(x,t)dx+V=\rho A dx \frac{\partial^2 w(x,t)}{\partial t^2}, \quad (1)$$

Where ρ is the mass density and is the cross – sectional area of the beam. The moment equation about the y axis leads to:

$$(M+dM)-(V+dV)dx+f(x,t)dx\frac{dx}{2}-M-N\left(U+\Delta U-U\right)=0 \quad (2)$$

$$dV=\frac{\partial V}{\partial x}dx \text{ and } dM=\frac{\partial M}{\partial x}dx \quad (3)$$

And neglecting higher powers of dx , the equations 2 and 3 can be written as:

$$-\frac{\partial V(x,t)}{\partial x}+f(x,t)=\rho A\frac{\partial^2 U(x,t)}{\partial t^2} \quad (4)$$

$$\frac{\partial M(x,t)}{\partial x}-V(x,t)-N\frac{\partial U}{\partial x}=0 \quad (5)$$

© JUL 2026 | IRE Journals | Volume 10 Issue 1 | ISSN: 2456-8880
DOI: https://doi.org/10.64388/IREV10I1-1719856

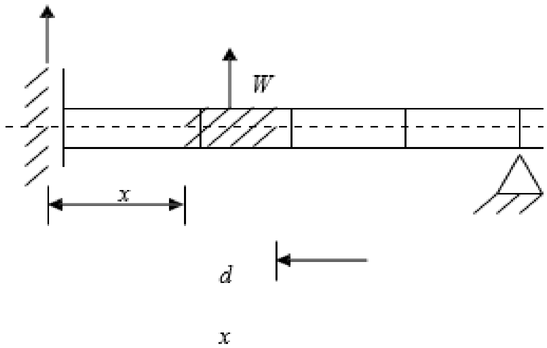

Fig. 1. A beam under transverse vibration

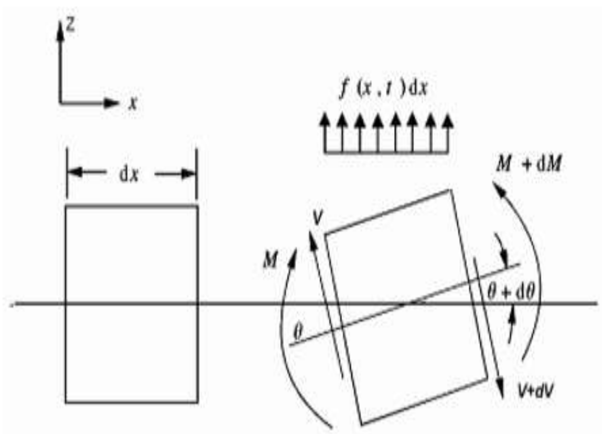

Fig. 2. Free body diagram of a section of a beam under transverse vibration

Figure 1 presents a schematic representation of a beam subjected to transverse vibration, a scenario commonly encountered in structural and transportation engineering. The beam is supported in such a way that its left end is fixed, restricting both vertical displacement and rotation, while the right end is simply supported, permitting rotation but not vertical movement. This configuration is typical in practical engineering applications where structures experience varying support conditions. A concentrated load, denoted by W, is applied at a specific location on the beam and is shown moving from left to right along the length of the beam. The position of this moving load at any time is indicated by the variable x, while d represents the direction of motion. This setup simulates the dynamic behavior of the beam under the influence of a moving force or mass, such as a vehicle crossing a bridge or a trolley moving along a track. The transverse vibration resulting from the moving load introduces deflections in the beam, which vary with time and the position of the load. This figure forms the basis for analyzing how different parameters, such as the speed, magnitude, and nature of the moving load (force or mass), affect the dynamic response of the beam. Such analysis is crucial for ensuring the structural integrity and performance of components in systems like railways, bridges, and mechanical assemblies.

Figure 2 presents a detailed free body diagram of a small section of a beam undergoing transverse vibration. This diagram is foundational for deriving the equations of motion used in analyzing beam dynamics under varying load conditions. The beam element is shown with a differential length dx, isolated to study the internal forces and moments acting on it. The coordinate axes indicate that the beam lies along the horizontal x-axis, while the transverse displacement occurs along the vertical z-axis. A distributed load $f\ (x,\ t)\ dx$ acts vertically on the element, representing a time- and position-dependent external force such as a moving load or an oscillatory excitation. To understand the internal stress state of this beam section, the diagram shows the shear force V and bending moment M acting on the left face of the element. On the right face, these quantities increase incrementally to $V + dV$ and $M + dM$, respectively, accounting for changes along the beam's length. The rotation of the beam element is denoted by the angular displacement θ, which increases by an infinitesimal amount $d\theta$ across the element, signifying bending deformation due to the applied load.

The combination of shear forces, bending moments, and angular rotation illustrates the dynamic behavior of the beam section, and the figure serves as a visual foundation for formulating the differential equations that govern the transverse vibration of beams.

By using the relation $V = \frac{\partial M}{\partial x}$ from above two equations:

$$-\frac{\partial^2 M(x,t)}{\partial x^2} + f(x,t) = \rho A \frac{\partial^2 U(x,t)}{\partial t^2} - N\frac{\partial^2 U}{\partial x^2}$$
(6)

© JUL 2026 | IRE Journals | Volume 10 Issue 1 | ISSN: 2456-8880
DOI: https://doi.org/10.64388/IREV10I1-1719856

From the elementary theory of bending of beam, the relationship between bending moment and deflection can be expressed as:

$$M(x,t) = EI\frac{\partial^2 U(x,t)}{\partial x^2} \quad (7)$$

where E is the Young's modulus and I is the variable moment of inertia of the beam cross section about the y axis. Inserting equation (7) into (6) for the forced transverse vibration of a uniform beam gives:

$$\frac{\partial^2}{\partial x^2}\left[EI\frac{\partial^2 U(x,t)}{\partial x^2}\right] + \rho A\frac{\partial^2 U(x,t)}{\partial t^2} - N\frac{\partial^2 U}{\partial x^2} = f(x,t)$$
(8)

For a uniform beam equation (8) reduces to:

$$EI\frac{\partial^4 U(x,t)}{\partial x^4} + \rho A\frac{\partial^2 U(x,t)}{\partial t^2} - N\frac{\partial^2 U}{\partial x^2} = f(x,t)$$
(9)

For free vibration $f(x,t) = 0$, and so the equation of motion becomes:

$$c^2\frac{\partial^4 U(x,t)}{\partial x^4} + \frac{\partial^2 U(x,t)}{\partial t^2} = 0 \quad (10a)$$

where:

$$c = \sqrt{\frac{El}{\rho A}} \quad (10b)$$

Equation (9) is the governing differential equation of the stressed Bernoulli beam and the external load $f(x,t)$ is considered to be concentrated moving load.

$$f(x,t) = Mg\delta(x-ct) - M\delta(x-ct)\left[\frac{\partial^2}{\partial t^2} + 2c\frac{\partial^2}{\partial x^2\partial t^2} + c^2\frac{\partial^2}{\partial x^2}\right]U(x,t) - KU(x,t) \quad (11)$$

The boundary condition for simply supported beam:

$$U(x,t)\big|_{x=x_e} = 0 \quad (12a)$$

And $M(x_e,t) = 0$ (12b)

This implies that the displacement and the bending moment varnish at a simply supported end from equation (12b) and (7), then the secondary condition is expressed in terms of U as $\left.\frac{\partial^2 U}{\partial x^2}\right|_{x=x_e} = 0$

Substituting equation (11) into (9) gives Oni and Awodola [57] the governing equation:

$$\frac{\partial^2}{\partial x^2}\left[EI\frac{\partial^2 U(x,t)}{\partial x^2}\right] + \mu\frac{\partial^2 U(x,t)}{\partial t^2} - N\frac{\partial^2 U(x,t)}{\partial x^2} + M\delta(x-ct)\left[\frac{\partial^2}{\partial t^2} + 2c\frac{\partial^2}{\partial x^2\partial t^2} + c^2\frac{\partial^2}{\partial x^2}\right]U(x,t) +$$

$$KU(x,t) = Mg\delta(x-ct) \quad (13)$$

The old model of Oni and Awodola [57] was modified by incorporating the variable Inertia and variable elastic k-stiffness instead of the usual constant Moment of Inertia and k-stiffness and the force was also taken to be partially distributed.

2.2 The New Model

In this new research work instead of the usual concentrated force, it going to consider being uniform distributed and the usual assumptions of constants moment of inertia and k-stiffness is going to be variable. The problem dynamic behavior of Euler bernoulli beam of arbitrary Number of variable elastic K-Stiffness under a partially distributed moving load is governed by the fourth order partial differential equation given by

$$\frac{\partial^2}{\partial x^2}\left[EI(x)\frac{\partial^2 U(x,t)}{\partial x^2}\right] + \mu(x)\frac{\partial^2 U(x,t)}{\partial x^2} - N(x)\frac{\partial^2 U(x,t)}{\partial t^2} + K(x)U(x,t) +$$

$$M\left[\frac{\partial^2}{\partial t^2}+2V\frac{\partial^2}{\partial x^2\partial t^2}+V^2\frac{\partial^2}{\partial x^2}\right]U(x,t)\left[H\left(x-\xi+\frac{\varepsilon}{2}\right)-H\left(x-\xi-\frac{\varepsilon}{2}\right)\right]=$$
$$U(L,t)=0=U''(L,t)$$
$$Mg\left[H\left(x-\xi+\frac{\varepsilon}{2}\right)-H\left(x-\xi-\frac{\varepsilon}{2}\right)\right] \quad (14)$$

Subject to the boundary and initial conditions below:

$$U(0,t)=0=U'(0,t)$$
$$U(L,t)=0=U''(L,t)$$
$$U(x,0)=\dot{U}(x,0) \quad (15)$$

where:
E is the Young's Modulus
$U(x,t)$ is the Transverse Displacement
$K(x)$ is the Variable Elastic K-Stiffness
$\mu(x)$ is the Variable Mass per unit Length of the Beam
$I(x)$ is the Variable Moment of Inertia,
$N(x)$ is the Pre - Stress
(x,t) Spatial and Time coordinates respectively

Assuming a constant below:

$$K(x)=K_0(1+4x-3x^2+x^3)$$
$$N(x)=I_0\left(1+\sin\frac{\pi x}{L}\right)$$
$$\mu(x)=\mu_0\left(1+\sin\frac{\pi x}{L}\right)$$
$$I(x)=I_0\left(1+\sin\frac{\pi x}{L}\right)^3=1+3\sin\frac{\pi x}{L}+3\sin^2\frac{\pi x}{L}+\sin^3\frac{\pi x}{L}$$
(16)

$$U(x,0)=\dot{U}(x,0)$$
$$U(x,0)=\dot{U}(x,0) \quad (17)$$

Where is elastic K-stiffness, I_0 and N_0 are taken to be constants.

Furthermore, we assume that the beam has simple supports at the end $x=0$ ***and at the end*** $x=L$. Therefore, the both the bending movement and the deflection vanish at both ends. Thus, the pertinent boundary conditions that pertain at these two ends is given as:

$$U(0,t)=0=U'(0,t)$$

Where
E is the Young's Modulus
$U(x,t)$ is the Transverse Displacement
$K(x)$ is the Variable Elastic Foundation
$\mu(x)$ is the Variable Mass per unit Length of the Beam
$I(x)$ is the Variable Moment of Inertia,
(x,t) Spatial and time coordinates, respectively

Assuming a constant:

$$K(x)=K_0(1+4x-3x^2+x^3)$$
$$N(x)=I_0\left(1+\sin\frac{\pi x}{L}\right)$$
$$\mu(x)=\mu_0\left(1+\sin\frac{\pi x}{L}\right)$$
$$I(x)=I_0\left(1+\sin\frac{\pi x}{L}\right)^3=1+3\sin\frac{\pi x}{L}+3\sin^2\frac{\pi x}{L}+\sin^3\frac{\pi x}{L}$$
(18)

Substituting equation (18) into equation (14) gives:

$$EI_0\frac{\partial^2}{\partial x^2}\left[\left(1+\sin\frac{\pi x}{L}\right)^3\frac{\partial^2 U(x,t)}{\partial x^2}\right]+\mu_0\left(1+\sin\frac{\pi x}{L}\right)\frac{\partial^2 U(x,t)}{\partial t^2}+K_0(1+4x-3x^2+x^3)U(x,t)-$$

$$N_0\left(1+\sin\frac{\pi x}{L}\right)\frac{\partial^2 U(x,t)}{\partial x^2}+M\left[\frac{\partial^2}{\partial t^2}+2V\frac{\partial^2}{\partial x^2\partial t^2}+V^2\frac{\partial^2}{\partial x^2}\right]U(x,t)\left[H\left(x-\xi+\frac{\varepsilon}{2}\right)-H\left(x-\xi-\frac{\varepsilon}{2}\right)\right]=$$

$$Mg\left[H\left(x-\xi+\frac{\varepsilon}{2}\right)-H\left(x-\xi-\frac{\varepsilon}{2}\right)\right] \quad (19)$$

© JUL 2026 | IRE Journals | Volume 10 Issue 1 | ISSN: 2456-8880
DOI: https://doi.org/10.64388/IREV10I1-1719856

On expanding, (18) result into:

$$\left(10+15\,sin\frac{\pi x}{L}-6cos\frac{2\pi x}{L}-sin\frac{3\pi x}{L}\right)\frac{\partial^4 U(x,t)}{\partial x^4}+$$
$$\left(\frac{30\pi}{L}cos\frac{\pi x}{L}+\frac{24\pi}{L}sin\frac{2\pi x}{L}-\frac{6\pi}{L}cos\frac{3\pi x}{L}\right)\frac{\partial^3 U(x,t)}{\partial x^3}+$$
$$\left(\frac{24\pi^2}{L^2}\cos\frac{2\pi x}{L}-\frac{15\pi}{L^2}\sin\frac{3\pi x}{L}+\frac{9\pi^2}{L^2}\sin\frac{\pi x}{L}\right)\frac{\partial^2 U(x,t)}{\partial x^2}+\mu_0\left(1+sin\frac{\pi x}{L}\right)\frac{\partial^2 U(x,t)}{\partial t^2}-$$
$$N_0\left(1+\sin\frac{\pi x}{L}\right)\frac{\partial^2 U(x,t)}{\partial x^2}+K_0(1+4x-3x^2+x^3)U(x,t)=$$
$$\left[Mg-M\left(\frac{\partial^2}{\partial t^2}+2V\frac{\partial^2}{\partial x^2\partial t^2}+V^2\frac{\partial^2}{\partial x^2}\right)U(x,t)\right]$$

(20)

Applying the orthogonality conditions below:

$$\int_0^L X_n(x)X_k(x)dx=\begin{cases}0, & n\neq k\\ \alpha & n=k\end{cases}$$

(21)

Solving equation (20) and apply the orthogonality condition the results we resulted in equation (22) and (23).

(a) Moving Force (Neglecting the inertia terms)

$$\left(P_{11}+P_{12}\right)\ddot{T}_n(t)+\left(P_1+P_2-P_3-P_4+P_5+P_6-P_7+P_8-P_9+P_{10}-P_{13}+P_{14}+P_{15}+P_{16}+P_{17}+P_{18}\right)T_n(t)=$$
$$P_{23}-P_{24} \qquad (22)$$

(b) If all inertia terms were taken into consideration, we have Moving Mass:

$$\left(P_{11}+P_{12}+P_{19}+P_{20}\right)\ddot{T}_n(t)+\left(P_{21}-P_{22}\right)\dot{T}_n(t)+$$

(23)

$$\left(P_1+P_2-P_3-P_4+P_5+P_6-P_7+P_8-P_9+P_{10}-P_{13}+P_{14}+P_{15}+P_{16}+P_{17}+P_{18}+P_{23}-P_{24}\right)T_n(t)=P_{25}-P_{26}$$

III. RESULTS

3.1 Numerical Results and Discussion

For numerical analysis, the numerical values were assigned as follows:

$L=10m,\ M=3kg\ 6kg\ 9kg,\ \mu=75kg/m,$
$E=2.07\times10^{-19}N/m^2,\qquad \varepsilon=0.1,$
$I=1.04\times10^{-6}m^4,\ \ \nu=3.3m/s,\ \ g=10ms^{-2},$
$\pi=3.14,\ \ n=1,2,3\ldots$

The transverse deflections of the beam are calculated and tabulated against time for various values of moving load and subgrade K, values of K between 0 and 50000 where used. The results are shown in the various Table below. Table 1 displays the Moving Load and Force at different values of Elastic K-stiffness and the results show that as the Elastic K-stiffness increases, while displacement of the beam decreases. It displays the Moving Force at different values of Elastic K-stiffness, the results show that as the Elastic K-stiffness increases, while the displacement of the beam decreases.

Table 1. Moving load and force at different value of Elastic K-stiffness

t(sec)	Moving Load W(x, t) K=0	W(x, t) K=50000	W(x, t) K=60000	Moving Force W(x, t) K=0	W(x, t) K=50000	W(x, t) K=60000
0	0.00E+00	0.00E+00	0.00E+00	0.00E+00	0.00E+00	0.00E+00
0.01	7.62E-10	7.62E-08	2.59E-09	3.81E-08	3.81E-08	1.29E-09
0.02	1.51E-7	1.51E-07	9.98E-09	7.56E-08	7.57E-08	4.99E-09
0.03	7.41E-8	7.41E-08	2.12E-08	3.70E-08	3.71E-08	1.06E-08
0.04	1.09E-10	1.10E-10	3.46E-08	5.48E-11	5.48E-11	1.73E-08
0.05	7.83E-8	7.83E-08	4.85E-08	3.91E-08	3.92E-08	2.43E-08

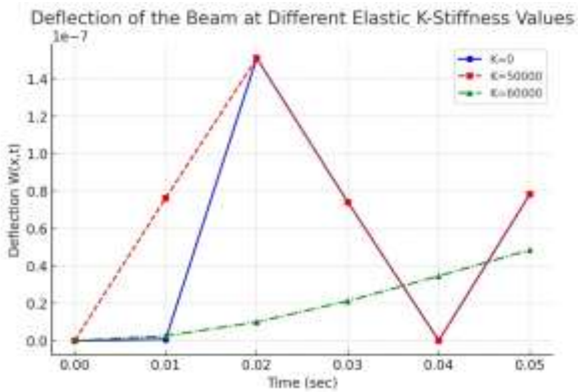

Fig. 3. Deflection of a beam subjected to a moving load under different values of elastic K-stiffness (K = 0, K = 50000, and K = 60000)

Figure 3 illustrates the deflection of a beam subjected to a moving load under different values of elastic K-stiffness (K = 0, K = 50000, and K = 60000). The results show that the beam's deflection varies significantly depending on the stiffness, highlighting the role of structural elasticity in dynamic response. For K = 50000, the beam experiences the highest deflection, peaking around t = 0.02 seconds. This suggests that at this intermediate stiffness level, the structure exhibits a more pronounced deformation under the moving load. In contrast, when K = 60000, the deflection remains lower throughout the time interval, indicating that higher stiffness provides greater resistance to deformation. The case where K = 0 follows a similar pattern to K = 50000, but with a lower peak deflection, implying that the absence of stiffness still allows for some flexibility in the beam's response. Over time, the deflection pattern varies with stiffness. For K = 50000, the beam deflects sharply, reaching its maximum displacement at t = 0.02 seconds before decreasing and exhibiting another rise at t = 0.05 seconds.

In contrast, the K = 60000 scenario results in a more gradual increase in deflection, demonstrating that higher stiffness dampens oscillations and leads to a more controlled response. The K = 0 case follows an increasing trend initially, peaking at t = 0.02 seconds, but does not reach the same magnitude as K = 50000. Structurally, these results suggest that an intermediate stiffness value (K = 50000) may lead to the most significant displacement, which could have implications for material selection and structural design. A very high stiffness value (K = 60000) minimizes deflection, making the beam more resistant to deformation but potentially affecting its ability to absorb dynamic loads. Thus, balancing stiffness is crucial in optimizing the structural performance of beams under moving loads.

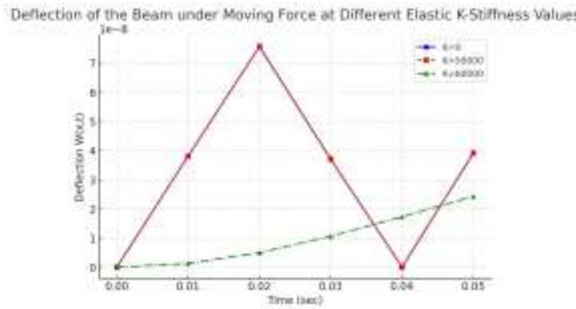

Fig. 4. Deflection response of a beam under a moving force at different elastic K-stiffness values over time

Figure 4 illustrates the deflection response of a beam under a moving force at different elastic K-stiffness values over time. The x-axis represents time (t) in seconds, while the y-axis denotes the beam's deflection $W(x, t)$, with values scaled to 10^{-8}. This visualization compares the deflection behavior for three distinct stiffness values: K = 0, K = 50000, and K = 60000, highlighting how stiffness influences structural deformation when subjected to a moving force. From the plot, it is evident that stiffness significantly affects the beam's deflection. The curve for K = 50000 (represented by the red line) exhibits the highest deflection peaks, indicating that under this stiffness condition, the beam undergoes substantial deformation in response to the applied force. The sharp rise and fall in deflection suggest that the structure experiences resonance effects at certain time intervals, which could lead to structural instability if not properly managed.

In contrast, the curve for K = 60000 (green line) demonstrates a more gradual increase in deflection over time, implying that higher stiffness helps to mitigate abrupt fluctuations and stabilize the structural response. This suggests that increasing the stiffness of the beam can enhance its resistance to deformation under dynamic loads. Additionally, the blue curve representing K = 0 follows a similar trend to K = 50000 but with a lower magnitude of

© JUL 2026 | IRE Journals | Volume 10 Issue 1 | ISSN: 2456-8880
DOI: https://doi.org/10.64388/IREV10I1-1719856

deflection. This indicates that while the structure still experiences movement under the applied force, the absence of stiffness makes it more flexible, allowing for some level of energy dissipation rather than amplifying oscillations. A notable observation is the peak deflection occurring at t = 0.02 seconds for K = 50000, reaching approximately 7 × 10^{-8}. This suggests that at this moment, the moving force exerts maximum impact on the beam. Following this, there is a rapid decrease in deflection at t = 0.04 seconds, which could be attributed to a redistribution of the applied force or a shift in the load position.

Thus, this analysis aligns with the broader study of moving load problems in structural dynamics, where variations in stiffness play a crucial role in determining the stability and resilience of beam-type structures. The findings emphasize the need for optimizing stiffness parameters to balance flexibility and stability in engineering applications such as bridges, highways, and railway tracks subjected to moving loads.

Table 2 displays the Moving Load at different values of Masses for elastic K-stiffness; the results show that as the Moving Load increases, the mass is also increases. It also displays the Moving Force at different values of masses for Elastic Foundation; the results show that as the Moving Load increases, the mass also increases.

Table 2. Moving load and force at different Masses for Elastic K-stiffness

	Moving load			Moving force		
t(sec)	W(x, t), M=3kg	$W(x, t)$ M=6kg	$W(x, t)$ M=9kg	W(x, t), M=3kg	$W(x, t)$ M=6kg	$W(x, t)$ M=9kg
0	0.00E+00	0.00E+00	0.00E+00	0.00E+00	0.00E+00	0.00E+00
0.01	3.81E-08	7.77E-08	7.77E-08	7.62E-08	1.55E-07	2.37E-07
0.02	7.57E-08	1.51E-07	1.51E-07	1.51E-07	3.02E-07	4.53E-07
0.03	3.71E-08	6.99E-08	6.99E-08	7.41E-08	1.40E-07	1.97E-07
0.04	5.48E-11	5.62E-10	5.62E-10	1.10E-10	1.12E-09	4.28E-09
0.05	3.92E-08	8.54E-08	8.54E-08	7.83E-08	1.71E-07	2.77E-07

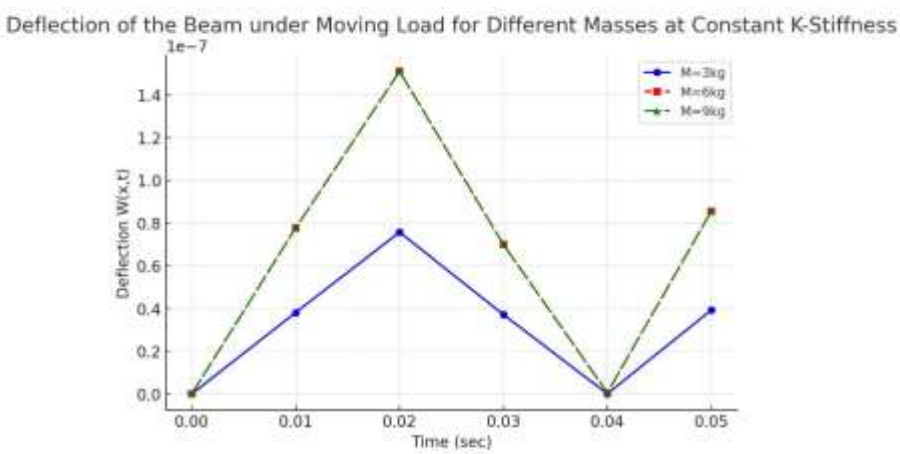

Fig. 5. Deflection of a beam subjected to a moving load for different masses while maintaining a constant K-stiffness

© JUL 2026 | IRE Journals | Volume 10 Issue 1 | ISSN: 2456-8880
DOI: https://doi.org/10.64388/IREV10I1-1719856

Figure 5 illustrates the deflection of a beam subjected to a moving load for different masses while maintaining a constant K-stiffness. The x-axis represents time (t) in seconds, and the y-axis shows the beam's deflection $W(x,\ t)$ scaled to 10^{-7}. The analysis compares the beam's response for three different moving masses: M = $3kg$, M = $6kg$, and M = $9kg$. From the plot, it is evident that the deflection of the beam increases as the mass of the moving load increases. The blue curve (M = $3kg$) exhibits the lowest deflection values, indicating that a lighter load exerts a smaller impact on the beam. Conversely, the red (M = $6kg$) and green (M = $9kg$) curves display nearly identical trends, with the highest peak deflection occurring at t = 0.02 seconds. The near overlap of these two curves suggests that beyond a certain mass threshold, additional weight does not significantly alter the deflection behavior.

A notable pattern in the chart is the sharp increase in deflection leading up to t = 0.02 seconds, followed by an equally rapid decline. This peak corresponds to the moment when the dynamic effects of the moving load induce maximum displacement in the beam. At t = 0.04 seconds, the deflection returns to near zero before increasing again at t = 0.05 seconds, indicating a periodic structural response under the moving load. The results align with theoretical expectations in structural dynamics, where heavier moving loads cause greater deflection due to increased force application. The minimal difference between the M = $6kg$ and M = $9kg$ cases may indicate a limit beyond which further increases in mass do not proportionally influence deflection, possibly due to stiffness constraints or damping effects in the system. Hence, this analysis reinforces the importance of considering moving mass effects in structural design, particularly for bridges, highways, and rail tracks where varying loads interact dynamically with beam structures. Understanding these deflection patterns helps in optimizing stiffness parameters to enhance stability and structural integrity.

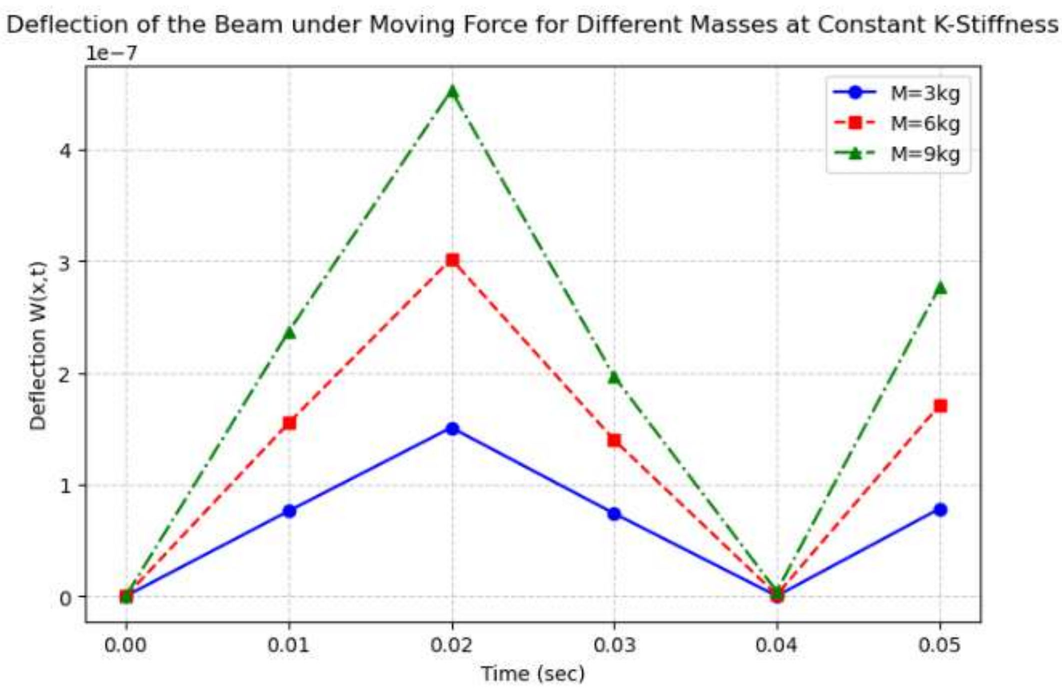

Fig. 6. Deflection of a beam under moving force for different mases at constant K-stiffness

© JUL 2026 | IRE Journals | Volume 10 Issue 1 | ISSN: 2456-8880
DOI: https://doi.org/10.64388/IREV10I1-1719856

Figure 6 illustrates the dynamic response of an Euler-Bernoulli beam subjected to a moving force corresponding to three different masses 3 kg, 6 kg, and 9 kg, while maintaining a constant elastic stiffness value (K). The deflection of the beam, denoted as $w(x, t)$, is plotted against time in seconds, ranging from 0 to 0.05 seconds. From the plot, it is evident that the deflection of the beam increases with the magnitude of the mass. At each observed time point, the largest deflection occurs with the 9 kg mass, followed by 6 kg and 3 kg respectively. This behavior is expected, as heavier moving forces exert greater influence on the structural response of the beam. The trajectory of each mass follows a similar temporal pattern, an increase in deflection from time zero to a peak at 0.02 seconds, followed by a sharp drop at 0.04 seconds, and then a modest rebound at 0.05 seconds. This trend highlights the oscillatory nature of the beam's response under dynamic loading, showcasing the influence of inertia and elastic rebound.

The symmetry and consistency in the shape of the curves across different mass values also suggest that the relationship between the applied moving force and beam deflection is linear under the examined conditions. Furthermore, the overall increase in deflection with mass supports the hypothesis that mass significantly contributes to the dynamic performance of structures under moving loads. This plot thus confirms the theoretical expectation that, for a beam of constant stiffness, increasing the magnitude of the moving force (via heavier mass) proportionally increases deflection, and that the beam undergoes time-dependent oscillations in response to such dynamic loading.

Table 3 displays the comparison of Moving Load and Moving Force for a particular value of Variable Elastic K-stiffness; the results show that the displacement of Moving Mass is more significant that of Moving Force

Table 3. Comparison of Moving Mass and Moving Force for variable K-stiffness (K = 0, K = 50000 and K = 60000)

t(sec)	Moving Mass K=0	Moving Force K=0	Moving Mass K=5000	Moving Force K=50000	Moving Mass K=60000	Moving Force K=60000
0	0.00E+00	0.00E+00	0.00E+00	0.00E+00	0.00E+00	0.00E+00
0.01	7.62E-10	3.81E-08	7.62E-08	3.81E-08	2.59E-09	1.29E-09
0.02	1.51E-7	7.56E-08	1.51E-07	7.57E-08	9.98E-09	4.99E-09
0.03	7.41E-8	3.70E-08	7.41E-08	3.71E-08	2.12E-08	1.06E-08
0.04	1.09E-10	5.48E-11	1.10E-10	5.48E-11	3.46E-08	1.73E-08
0.05	7.83E-8	3.91E-08	7.83E-08	3.92E-08	4.85E-08	2.43E-08
	t-stat = 0.688, p = 0.513		t-stat = 1.215, p = 0.2617		t-stat = 1.114, p = 0.300	

This study investigates how varying elastic stiffness parameters (denoted as K-stiffness) influence the dynamic response of a beam subjected to a moving load. The beam is modeled using the Euler-Bernoulli beam theory, which is commonly employed in the analysis of bending in beams under various loading conditions. The study specifically examines how the elastic stiffness (K) impacts the beam's behavior under different load distributions, particularly focusing on the moving load that is partially distributed along the beam. The varying K-stiffness values (K = 0, K = 50000, and K = 60000) represent different degrees of beam rigidity, which are expected to alter the beam's deflection, velocity, and acceleration profiles when subjected to the same moving load.

© JUL 2026 | IRE Journals | Volume 10 Issue 1 | ISSN: 2456-8880
DOI: https://doi.org/10.64388/IREV10I1-1719856

The results shown in Table 3 provide a comparison of the "Moving Mass" and "Moving Force" at these three different stiffness values (K = 0, K = 50000, and K = 60000) over a series of time intervals. The data for both "Moving Mass" and "Moving Force" are presented alongside the independent samples t-test results, which are used to determine if there are significant differences between the two variables at each stiffness level.

For K = 0, the t-statistic is 0.688 with a p-value of 0.513, which indicates that there is no significant difference between the "Moving Mass" and "Moving Force" at this level of stiffness. This suggests that, when the beam has no stiffness (K = 0), the moving mass and moving force exhibit similar behavior across the time intervals.

At K = 50000, the t-statistic is 1.215 with a p-value of 0.2617, indicating that there is still no significant difference between the moving mass and moving force at this stiffness level. Although the difference between the two variables is slightly more pronounced than at K = 0, it is not statistically significant, meaning the dynamic behavior of the beam at this stiffness level is still relatively similar for both moving mass and moving force.

For K = 60000, the t-statistic is 1.114 with a p-value of 0.300. Like the previous cases, the result suggests that there is no significant difference between the moving mass and moving force at this level of stiffness either. While there may be minor differences in the dynamic response as the stiffness increases, the overall behavior of the beam remains consistent across both variables.

Hence, the t-test results across all stiffness levels (K = 0, K = 50000, and K = 60000) indicate that there are no statistically significant differences between the "Moving Mass" and "Moving Force" under the given conditions. This suggests that, within the framework of the study, the dynamic behavior of the beam, as it relates to these two parameters, remains comparable regardless of the level of K-stiffness applied. Therefore, changes in K-stiffness do not appear to significantly alter the relative dynamics of mass and force in this particular case.

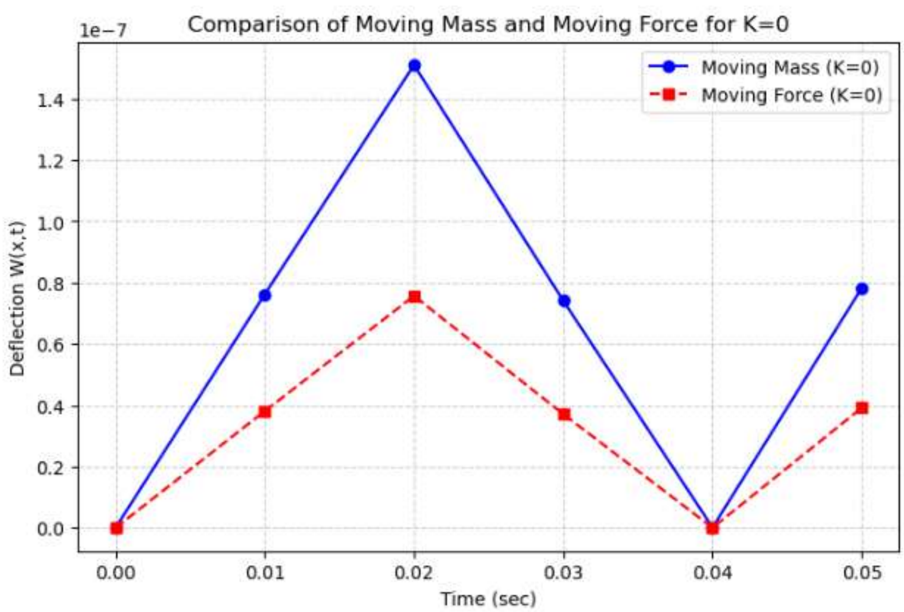

Fig. 7. Comparing of moving mass and moving force of a beam subjected to a moving load under elastic K-stiffness ($K = 0$)

© JUL 2026 | IRE Journals | Volume 10 Issue 1 | ISSN: 2456-8880
DOI: https://doi.org/10.64388/IREV10I1-1719856

Figure 7presents the time-dependent deflection of an Euler-Bernoulli beam subjected to two different types of loading, moving mass and moving force under a condition where the elastic stiffness $K = 0$, representing a theoretically flexible or extremely compliant beam. In this plot, the vertical axis shows the deflection $w(x, t)$, measured in units of 10^{-7}, while the horizontal axis represents time in seconds, ranging from 0 to 0.05. The blue solid line with circular markers indicates the deflection caused by a moving mass, while the red dashed line with square markers represents the deflection due to a moving force of the same magnitude. A key observation from the graph is that the beam subjected to a moving mass experiences significantly greater deflection at every time interval compared to the beam under a moving force. At the peak point (0.02 sec), the deflection due to the moving mass reaches approximately 1.5×10^{-7}, while the moving force produces just about half that amount ($\sim 0.75 \times 10^{-7}$). This difference underscores the greater dynamic impact of a moving mass, which incorporates both the inertial and gravitational effects, compared to the purely external application of a force.

Moreover, the pattern of deflection for both cases follows a similar trend—rising to a peak at 0.02 seconds, dipping to a minimum at 0.04 seconds, and then slightly rebounding at 0.05 seconds. However, the amplitude of oscillation is more pronounced for the moving mass, suggesting that the beam's response is more sensitive to inertial loading effects, especially when stiffness is absent or negligible. Thus, this chart confirms a critical finding in structural dynamics: that moving mass produces a more significant impact on beam deflection than an equivalent moving force. This insight is particularly important for the design and analysis of transportation infrastructure, such as railway bridges or vehicle-supported platforms, where the dynamic load may need to be modeled as a mass rather than a simple force for accurate assessment—especially in systems with low stiffness.

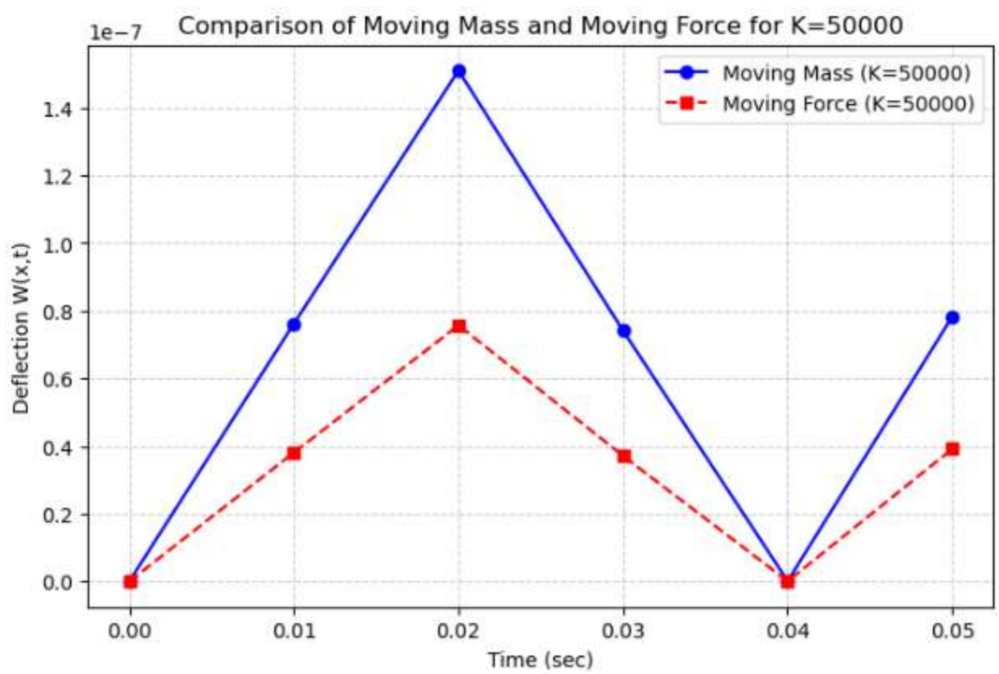

Fig. 8. Comparing of moving mass and moving force of a beam subjected to a moving load under elastic K-stiffness ($K = 50000$)

Figure 8 illustrates the deflection behavior of an Euler-Bernoulli beam subjected to two types of dynamic loads, moving mass and moving force, under a significantly stiffer condition, with the elastic stiffness coefficient $K = 50000$. The vertical axis represents the beam deflection $w(x, t)$ in units of 10^{-7}, while the horizontal axis shows time in seconds (from 0 to 0.05 seconds). The blue solid line with circular markers corresponds to the beam's response to a moving mass, while the red dashed line with square markers indicates the response to a moving force of equal magnitude. From the plot, it is evident that the beam continues to exhibit higher deflection under the moving mass across all time steps, even with the increased stiffness. At the peak point of 0.02 seconds, the deflection under moving mass reaches about 1.5×10^{-7}, while the deflection under moving force is slightly over 0.75×10^{-7}. This trend is consistent with previous observations where moving mass produces greater deformation due to the inclusion of inertial effects, as opposed to the externally applied moving force, which lacks mass-associated dynamics.

Interestingly, when compared to the earlier scenario where $K = 0$, the magnitude of deflection in both cases is significantly reduced. This demonstrates the expected mechanical behavior that increasing the beam's stiffness results in lower structural deformation under the same loading conditions. Thus, the stiffness parameter K plays a critical role in controlling the beam's displacement response. Another notable feature is the symmetry in the deflection patterns for both types of loading. The curves for both moving mass and force display a rise to a peak at 0.02 seconds followed by a dip at 0.04 seconds, which then slightly rises again at 0.05 seconds, indicating a similar temporal response pattern. However, the difference in magnitude confirms that even under stiff conditions, mass effects must not be ignored in accurate dynamic load modeling. Hence, the chart reinforces the importance of accounting for the dynamic nature of loads, particularly the inclusion of mass in beam modeling. It also highlights the effectiveness of stiffness as a mitigating factor for deflection. These findings have practical implications for structural design in transport systems such as railway tracks and bridges, where understanding the dynamic impact of moving vehicles is crucial for ensuring stability and service life.

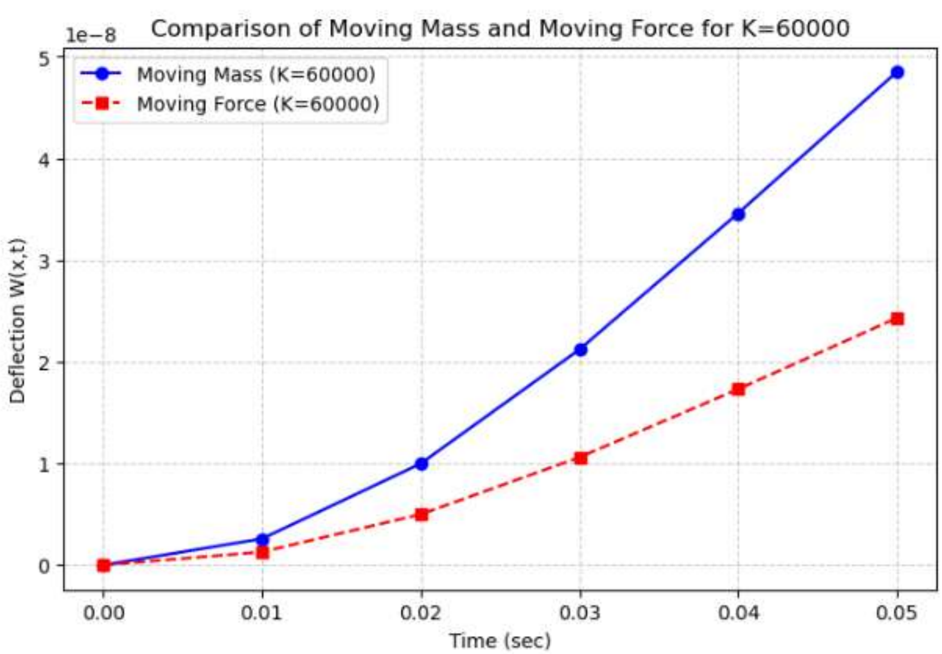

Fig. 9. Comparing of moving mass and moving force of a beam subjected to a moving load under elastic K-stiffness ($K = 60000$)

Figure 9 illustrates the time-dependent deflection behavior of an Euler-Bernoulli beam subjected to a moving load under a high elastic stiffness value. The analysis compares two distinct loading conditions: a moving mass and a moving force. The deflection $w(x, t)$, measured on the vertical axis in scientific notation ($\times 10^{-8}$), is plotted against time (in seconds) on the horizontal axis, covering a short dynamic interval from 0 to 0.05 seconds. From the chart, it is evident that the deflection of the beam increases steadily over time for both loading conditions. However, the rate and magnitude of deflection vary significantly between the two. The blue solid line with circular markers represents the response of the beam to a moving mass, while the red dashed line with square markers depicts the response to a moving force. Across the entire time interval, the deflection induced by the moving mass is consistently higher than that caused by the moving force. For example, at the final time point (0.05 seconds), the deflection due to the moving mass approaches approximately 5×10^{-8}, whereas the deflection under the moving force condition reaches about 2.5×10^{-8}.

This difference becomes more prominent as time progresses, indicating that the inertia effects associated with the moving mass play a significant role in influencing the structural response. The beam, although characterized by a relatively high stiffness (K = 60000), still exhibits notable sensitivity to the dynamic effects introduced by the moving mass. This contrasts with the moving force scenario, which does not account for the inertial interaction between the structure and the moving body. Furthermore, the smooth and monotonic increase in deflection for both cases suggests that the beam does not experience resonance or oscillatory instability within the observed time frame. This behavior differs from earlier observations under lower stiffness values, where deflections often followed more fluctuating or oscillatory patterns. The high stiffness of the beam in this case likely contributes to its damped, more controlled response. Thus, this chart reinforces the conclusion that the inclusion of mass in moving load problems significantly amplifies beam deflection, especially under conditions of high stiffness. It highlights the importance of accounting for moving mass effects in structural dynamics analysis, particularly in high-speed transportation systems or precision structural components where accurate deflection prediction is critical for safety and performance.

IV. CONCLUSION

This study delved into the dynamic behavior of an Euler-Bernoulli beam subjected to a partially distributed moving load, with a focus on varying elastic stiffness (K) values. Numerical solutions were obtained using Maple 16 by reducing the governing fourth-order partial differential equation to a second-order ordinary differential equation through an analytical series solution approach. The findings indicate that beam displacement decreases as the elastic stiffness (K) increases, while an increase in moving mass (M) results in greater displacement. Comparative analysis between the Moving Force and Moving Mass models revealed that the Moving Mass model predicts more significant displacements, attributed to the inclusion of inertial effects. These observations align with existing literature. For instance, Chawla and Pakrashi [56] examined the dynamic response of an Euler-Bernoulli beam on a two-parameter Pasternak foundation under both moving load and moving mass scenarios. Their results demonstrated that the Moving Mass model induces higher deflections due to the additional inertial forces introduced by the moving mass.

Similarly, Esen [58] investigated the dynamic behavior of a beam carrying an accelerating moving mass using a moving finite element approximation. The study highlighted that considering the inertial effects of the moving mass is crucial for accurately predicting the beam's dynamic response. Furthermore, Akinpelu [59] analyzed the response of a viscously damped Euler-Bernoulli beam to uniform partially distributed moving loads. The study found that the response amplitude due to the moving force is greater than that due to the moving mass, underscoring the importance of incorporating damping effects in dynamic analyses. Additionally, research by Rajib et al. [60] on beams supported by Pasternak foundations subjected to moving loads emphasized the significant role of foundation stiffness parameters in influencing beam deflections.

© JUL 2026 | IRE Journals | Volume 10 Issue 1 | ISSN: 2456-8880
DOI: https://doi.org/10.64388/IREV10I1-1719856

The statistical analysis conducted in this study, yielding a t-statistic of 1.215 and a p-value of 0.2617, suggests no significant difference between the Moving Force and Moving Mass models at K = 5000.

This finding is consistent with the work of Mofid [61], who demonstrated that the responses of structures due to moving mass must be properly accounted for, as they often differ significantly from the moving force model. Graphical representations from this study further illustrate that increased beam stiffness leads to reduced deformation, while higher moving masses result in larger deflections due to increased dynamic load intensity. These results corroborate the conclusions drawn in previous research [62-64], reinforcing the importance of accounting for both elastic stiffness and inertial effects in the dynamic analysis of beam structures under moving loads. In summary, this study contributes to the body of knowledge by providing a comprehensive analysis of beam deflections under dynamic loading conditions, emphasizing the interplay between elastic stiffness and moving mass. The findings have practical implications for the design and optimization of structural elements in engineering applications subjected to dynamic loading, such as bridges, railways, and runways.

V. POLICY IMPLICATIONS AND RECOMMENDATIONS

The findings of this study have significant implications for transportation infrastructure, particularly in the design and maintenance of railway tracks, bridges, and highways subjected to moving loads. The results demonstrate that incorporating the effects of moving mass, rather than relying solely on moving force models, provides a more accurate prediction of structural responses. This has direct policy implications for engineering standards, as current design codes should consider the influence of moving mass and elastic stiffness to enhance structural resilience and longevity.

To improve the safety and durability of transportation infrastructure, policymakers should mandate dynamic analyses that incorporate variable stiffness and mass effects in structural design. Additionally, transportation agencies should invest in advanced computational tools and numerical modeling techniques to optimize beam structures under dynamic loading conditions. Future research should also explore real-time monitoring systems for bridges and railway tracks to assess dynamic responses and prevent structural failures. Also, future research could extend this analysis to nonlinear beam models, different boundary conditions, and varying velocity profiles to capture more complex real-world scenarios.

REFERENCES

[1] Asiri SA. Dynamic, fatigue and harmonic analysis of a beam to beam system with various cross-sections under impact load. Heliyon. 2022;8(9):e10466. https://doi.org/10.1016/j.heliyon.2022.e10466

[2] Zamani Nejad M, Hadi A. Non-local analysis of free vibration of bi-directional functionally graded Euler–Bernoulli nano-beams. Int J Eng Sci. 2016;105:1–11. https://doi.org/10.1016/j.ijengsci.2016.06.003

[3] Corrêa RT, Simões FMF, da Costa AP. Moving loads on beams on Winkler foundations with passive frictional damping devices. Eng Struct. 2017;152:191–202. https://doi.org/10.1016/j.engstruct.2017.09.023

[4] Lei T, Zheng Y, Yu R, Yan Y, Xu B. Dynamic response of slope inertia-based Timoshenko beam under a moving load. Appl Sci. 2022;12(6):3045. https://doi.org/10.3390/app12063045

[5] Molina-Villegas JC, Ballesteros Ortega JE, Ruiz Cardona D. Formulation of the Green's functions stiffness method for Euler–Bernoulli beams on elastic Winkler foundation with semi-rigid connections. Eng Struct. 2022;266:114616. https://doi.org/10.1016/j.engstruct.2022.114616

[6] Autengruber M, Lukacevic M, Wenighofer G, Mauritz R, Füssl J. Finite-element-based concept to predict stiffness, strength, and failure of wood composite I-joist beams under various loads and climatic conditions. Eng Struct. 2021;245:112908. https://doi.org/10.1016/j.engstruct.2021.112908

[7] Turkyilmazoglu M. Uniformly loaded logarithmic beam mode with spatially varying flexural rigidity. Arab J Sci Eng. 2025;50:2823–33. https://doi.org/10.1007/s13369-024-09275-0

[8] Froio D, Verzeroli L, Ferrari R, et al. On the numerical modelization of moving load beam problems by a dedicated parallel computing FEM implementation. Arch Computat Methods Eng. 2021;28:2253–314. https://doi.org/10.1007/s11831-020-09459-5

[9] Jindal S, Rahmanli U, Aleem M, Cui L, Bhattacharya S. Geotechnical challenges in monopile foundations and performance assessment of current design methodologies. Ocean Eng. 2024;310(Part 1):118469. https://doi.org/10.1016/j.oceaneng.2024.118469

[10] Gbadeyan JA, Hammed FA. Influence of a moving mass on the dynamic behaviour of viscoelastically connected prismatic double-Rayleigh beam system having arbitrary end supports. Chin J Math. 2017. https://doi.org/10.1155/2017/6058035

[11] Rajabi K, Li L, Hosseini-Hashemi S, Nezamabadi A. Size-dependent nonlinear vibration analysis of Euler–Bernoulli nanobeams acted upon by moving loads with variable speeds. Mater Res Express. 2018;5(1):015058. https://doi.org/10.1088/2053-1591/aaa6e9

[12] Chemami A, Khadri Y, Tekili S, Daya EM, Daouadji A, et al. Damped dynamic response of strengthened beams by composite coats under moving force by FEM. Matériaux et Techniques. 2018;106(2):206. https://doi.org/10.1051/mattech/2018025

[13] AlSaleh R, Nasir A, Abu-Alshaikh I. Investigating fractional damping effect on Euler–Bernoulli beam subjected to a moving load. Shock Vib. 2023;2023:9524177. https://doi.org/10.1155/2023/9524177

[14] Migliaccio G, Ferretti M, Di Nino S, Luongo A. Analytical prediction of the dynamics of beams under traveling loads and external resonance phenomena. J Sound Vib. 2024;593:118656. https://doi.org/10.1016/j.jsv.2024.118656

[15] Togun N, Bağdatli SM. Application of modified couple-stress theory to nonlinear vibration analysis of nanobeam with different boundary conditions. J Vib Eng Technol. 2024;12:6979–7008. https://doi.org/10.1007/s42417-024-01294-3

[16] Zhang B, Kou Y, Jin K. Dynamic behavior of beam with an elastic foundation under the extended moving load for electromagnetic launch rail-structure. J Sound Vib. 2025;596:118756. https://doi.org/10.1016/j.jsv.2025.118756

[17] Oladazimi M, Putelat T, Szalai R, et al. Conveyance of texture signals along a rat whisker. Sci Rep. 2021;11:13570. https://doi.org/10.1038/s41598-021-92770-3

[18] Ali S, Hawwa M. Dynamics of axially moving beams: A finite difference approach. Ain Shams Eng J. 2022. https://doi.org/10.1016/j.asej.2022.101817

[19] Sali M, Fabien K, Bertin NJ, Njifenjou A. Numerical study of the vibrations of beams with variable stiffness under impulsive or harmonic loading. World J Eng Technol. 2024;12(2):401–25. https://doi.org/10.4236/wjet.2024.122026

[20] Fang J, Xiao Z, Zhu X, You L, Wang X, Zhang J. Fast and compact partial differential equation (PDE)-based dynamic reconstruction of extended position-based dynamics (XPBD) deformation simulation. Mathematics. 2024;12(20):3175. https://doi.org/10.3390/math12203175

[21] Tran-Duc T, Bunder JE, Roberts AJ. Efficient prediction of static and dynamical responses of functional graded beams using sparse multiscale patches. Comput Mech. 2025. https://doi.org/10.1007/s00466-025-02614-4

[22] Li J, Zhang H. Moving load spectrum for analyzing the extreme response of bridge free vibration. Shock Vib. 2020;2020:9431620. https://doi.org/10.1155/2020/9431620

[23] Xu X, Wang Y. Vibration control of AFG beam with moving load in thermal environment. Materials. 2025;18(3):725. https://doi.org/10.3390/ma18030725

[24] Bîrsan M, Pietras D, Sadowski T. Determination of effective stiffness properties of multilayered composite beams. Continuum Mech Thermodyn. 2021;33:1781–803. https://doi.org/10.1007/s00161-021-01006-2

[25] Sali M, Fabien K, Bertin NJ, Njifenjou A. Numerical study of the vibrations of beams with variable stiffness under impulsive or harmonic loading. World J Eng Technol. 2024;12(2):401–25. https://doi.org/10.4236/wjet.2024.122026

[26] Chanda AG, Ojo SO, Oliveri V, Weaver PM. Dynamic analysis of variable stiffness curved composite beams based on the inverse differential quadrature method. Composite Struct. 2025;363:119087. https://doi.org/10.1016/j.compstruct.2025.119087

[27] Pradhan PK, Sarangi SK. Free vibration analysis of functionally graded beams by finite element method. IOP Conf Ser: Mater Sci Eng. 2018;377(1):012211. https://doi.org/10.1088/1757-899X/377/1/012211

[28] Botis M, Imre L, Conțiu M. Numerical method of increasing the critical buckling load for straight beam-type elements with variable cross-sections. Appl Sci. 2023;13(3):1460. https://doi.org/10.3390/app13031460

[29] Al Mahmoud Z, Safaei B, Sahmani S, et al. Computational linear and nonlinear free vibration analyses of micro/nanoscale composite plate-type structures with/without considering size dependency effect: A comprehensive review. Arch Computat Methods Eng. 2025;32:113–232. https://doi.org/10.1007/s11831-024-10132-4

[30] Qiao G, Rahmatalla S. Moving load identification on Euler-Bernoulli beams using modal acceleration response. Comput Methods Appl Mech Eng. 2023;394:115810. https://doi.org/10.1016/j.cma.2022.115810

[31] Manolis GD, Dadoulis GI. Passive control in a continuous beam under a traveling heavy mass: Dynamic response and experimental verification. Sensors. 2024;24(2):573. https://doi.org/10.3390/s24020573

[32] Shao M, Ma C, Hu S, Sun C, Jing D. Effects of time-varying fluid on dynamical characteristics of cantilever beams: Numerical simulations and experimental measurements. Math Probl Eng. 2020;2020:6679443. https://doi.org/10.1155/2020/6679443

[33] Lai Z, Jiang L, Zhou W. An analytical study on dynamic response of multiple simply supported beam system subjected to moving loads. Shock Vib. 2018;2018:2149251. https://doi.org/10.1155/2018/2149251

[34] van Dieën JH, Reeves NP, Kawchuk G, van Dillen LR, Hodges PW. Motor control changes in low back pain: Divergence in presentations and mechanisms. J Orthop Sports Phys Ther. 2019;49(6):370–9. https://doi.org/10.2519/jospt.2019.7917

[35] Pourzeynali S, Zhu X, Ghari Zadeh A, Rashidi M, Samali B. Comprehensive study of moving load identification on bridge structures using the explicit form of Newmark-β method: Numerical and experimental studies. Remote Sens. 2021;13(12):2291. https://doi.org/10.3390/rs13122291

[36] Shafiei B. Investigating the impact of the velocity of a vehicle with a nonlinear suspension system on the dynamic behavior of a Bernoulli–Euler bridge. SN Appl Sci. 2021;3(1):293. https://doi.org/10.1007/s42452-021-04280-6

[37] Phadke H, Jaiswal O. Dynamic analysis of railway track on variable foundation under harmonic moving load. Proc Inst Mech Eng Part F J Rail Rapid Transit. 2021;236(3):302–16. https://doi.org/10.1177/09544097211020838

[38] Yang S, Hu A, Mo G, Zhang J, et al. Dynamic modeling and analysis of an axially moving and spinning Rayleigh beam based on a time-varying element. Appl Math Model. 2021;95:1–17. https://doi.org/10.1016/j.apm.2021.01.049

[39] Pourzeynali S, Zhu X, Ghari Zadeh A, Rashidi M, Samali B. Simultaneous identification of bridge structural damage and moving loads using the explicit form of Newmark-β method: Numerical and experimental studies. Remote Sens. 2022;14(1):119. https://doi.org/10.3390/rs14010119

[40] Panda S, Banerjee A, Manna B. Effectiveness of an elastically supported beam under the action of moving loads traversing in the opposite direction. J Vib Control. 2023;30(9–10):2093–110. https://doi.org/10.1177/10775463231174661

[41] Fu J, Yu Z, Guo Q, Zheng L, Gan D. A variable stiffness robotic gripper based on parallel beam with vision-based force sensing for flexible grasping. Robotica. 2023:1–19. https://doi.org/10.1017/S026357472300156X

[42] Pan Q, Zhang B, Gao C, Liu X. Experimental and analytical study on dynamic response of foundation beam with local void under moving load. Soil Dyn Earthq Eng. 2025;192:109312. https://doi.org/10.1016/j.soildyn.2025.109312

[43] Awodola TO, Jimoh SA, Awe BB, Okoubi E. Modelling dynamic responses of clamped non-uniformly prestressed Bernoulli-Euler beams on variable elastic foundations. Afr J Math Stat Stud. 2025;8(1):139–58. https://doi.org/10.52589/AJMSS-SRIJ0ROR

[44] Vashishtha G, Chauhan S, Singh R, Singh M, Tejani GG. A review of numerical techniques for frictional contact analysis. Lubricants. 2025;13(1):18. https://doi.org/10.3390/lubricants13010018

[45] Marzec I, Tejchman J. Experimental and numerical investigations on RC beams with stirrups scaled along height or length. Eng Struct. 2022;252:113621. https://doi.org/10.1016/j.engstruct.2022.113621

[46] Moshiri N, Martinelli E, Breveglieri M, Czaderski C. Experimental tests and numerical simulations on the mechanical response of RC slabs externally strengthened by passive and prestressed FRP strips. Eng Struct. 2023;292:116559. https://doi.org/10.1016/j.engstruct.2023.116559

[47] Oni ST, Ayankop-Andi E. On the response of a simply supported non-uniform Rayleigh beam to travelling distributed loads. J Niger Math Soc. 2017;36(2):435–57.

[48] Sarvestan V, Mirdamadi HR, Ghayour M. Vibration analysis of cracked Timoshenko beam under moving load with constant velocity and acceleration by spectral finite element method. Int J Mech Sci. 2017;122:318–30. https://doi.org/10.1016/j.ijmecsci.2017.01.008

[49] Usman MA, Hammed FA, Ogunwobi ZO, Okusaga ST. Dynamic response of Rayleigh beam on Winkler foundation subjected to partially distributed moving load. LAUTECH J Eng Technol. 2018;12(2):107–22.

[50] Ogunbamike OK, Oni ST. Flexural vibration to partially distributed masses of non-uniform Rayleigh beam resting on Vlasov foundation with general boundary conditions. J Niger Math Soc. 2019;38(1):55–88.

[51] Simões FMF, Pinto da Costa A. Finite element steady-state solution of a beam on a frictionally damped foundation under a moving load. Int J Non-Linear Mech. 2019;117:103247. https://doi.org/10.1016/j.ijnonlinmec.2019.103247

[52] Reiterer M, Strauss A, Täubling B, Frangopol DM. Vehicle impacts on reinforced concrete railway bridges. In: Jensen F, Frangopol M, Schmidt A, editors. Bridge Maintenance, Safety, Management, Digitalization and Sustainability. 1st ed. London: Taylor & Francis; 2024. ISBN: 978-1-032-77040-6.

[53] Kumar S, Nallasivam K. Dynamic response of a PSC box-girder bridge impacted by high-speed train load using the finite element approach. Innov Infrastruct Solut. 2025;10(1):22. https://doi.org/10.1007/s41062-024-01845-3

[54] Katsimpini P, Papagiannopoulos G, Hatzigeorgiou G. An in-depth analysis of the seismic performance characteristics of steel-concrete composite structures. Appl Sci. 2025;15(7):3715. https://doi.org/10.3390/app15073715

[55] Qiao G, Rahmatalla S. Dynamics of Euler-Bernoulli beams with unknown viscoelastic boundary conditions under a moving load. J Sound Vib. 2021;491:115771.

[56] Chawla R, Pakrashi V. Dynamic responses of a damaged double Euler-Bernoulli beam traversed by a ‘phantom’ vehicle. Struct Control Health Monit. 2022. https://doi.org/10.1002/stc.2933

[57] Oni ST, Awodola TO. Dynamic response under a moving load of an elastically supported non-prismatic Bernoulli-Euler beam on variable elastic foundation. Lat Am J Solids Struct. 2010;3:1–20.

[58] Esen İ. Dynamic response of a beam due to an accelerating moving mass using moving finite element approximation. Math Comput Appl. 2011;16(4):171–82. https://doi.org/10.3390/mca16010171

[59] Akinpelu FO. The response of viscously damped Euler-Bernoulli beam to uniform partially distributed moving loads. Appl Math. 2012;3(3):252–7.

[60] Rajabi K, Kargarnovin MH, Gharini M. Dynamic analysis of a functionally graded simply supported Euler–Bernoulli beam subjected to a moving oscillator. Acta Mech. 2013;224(2):425–46.

[61] Mofid M. Numerical solution for response of beams with moving mass. J Struct Eng. 1989;115(1):120–31.

[62] Idowu IA, Gbolagade AW, Olayiwola MO. On the response of loaded beam subjected to moving masses and external forces. Rep Opin. 2009;1(1).

[63] Idowu IA, Atilade AO, Okedeyi AS, Mustapha RA. Dynamic response of Euler-Bernoulli beam on variable pre-stressed under a partially distributed moving load. Niger J Phys. 2021;29(2).

[64] Idowu IA, Atilade AO, Okedeyi AS. Analysis of Bernoulli-Euler beam on variable K-stiffness subjected to partially distributed moving load. Niger J Phys. 2021;30(2).